



Proceedings of the Sixth International Conference on
Railway Technology: Research, Development and Maintenance
Edited by: J. Pombo
Civil-Comp Conferences, Volume 7, Paper 16.10
Civil-Comp Press, Edinburgh, United Kingdom, 2024
ISSN: 2753-3239, doi: 10.4203/ccc.7.16.10
©Civil-Comp Ltd, Edinburgh, UK, 2024

Research on the Modeling of Magnetic-Track Relations and Dynamic Performance of Superconducting Maglev Vehicle

J. Yang, S. Liu, J. Zhao, L. Dong and T. Han

**Maglev Research Institute,
CRRC Changchun Railway Vehicles Co., Ltd
China**

Abstract

Superconducting maglev systems have been developed as high-speed transportation systems. The magnetic-rail relation is an essential link between the maglev vehicle and the track and a crucial factor in ensuring the smooth and safe operation of the vehicle. In this paper, the circuit model based on superconducting maglev principle was used to developed to solve electromagnetic force. The magnetic-rail relation is then performed for the linear spring, nonlinear stiffness and coupling models. According to the dynamic simulations based on the new 200 m straight test line to research applicable conditions and accuracy of the three kinds of magnetic-rail relation models so as to further improve the efficiency of dynamic simulation of superconducting maglev vehicle.

Keywords: superconducting maglev vehicle, electromagnetic force characteristics, magnetic-track relation, dynamic simulation model, dynamic performance, test line dynamic test.

1 Introduction

Superconducting maglev is a type of maglev transportation system suitable for high-speed and ultra-high-speed operation. It is a passive self-stabilizing suspension system with the advantages of large suspension gap, strong line adaptation, high magnetic field strength, high traction efficiency and easy rescue. It was first proposed by Powell and Danby in 1966 [1], and then developed rapidly in Japan. Japan's superconducting maglev vehicle achieved a manned operation of 603km/h in 2015 [2], creating the

highest speed record of ground rail transit. At the same time, extensive dynamic line tests have further validated the technical feasibility of high-speed operation of superconducting maglev vehicle.

The electromagnetic force of superconducting maglev vehicle relies on superconducting magnet on the bogie and the levitation/guiding coils on the U-track. The electromagnetic interaction is simply referred to as the magnetic track relation. Therefore, the magnetic track relation is not only a crucial link between the vehicle system and the track system, but also a key factor in ensuring the safe and stable operation with excellent dynamic performance. Just like the research on magnetic track relation of EMS maglev [3], the magnetic track relation of superconducting maglev vehicle has been considered as the constant stiffness in the related fields at home and abroad [4-8]. In fact, this equivalence relation is the vertical and lateral decoupling of the magnetic track relation, which does not accurately describe the dynamic characteristics of the vehicle. However, during actual operation, the magnetic track relation is closely related to the fluctuations of the vehicle suspension and guide clearance.

This paper has carried out the modeling of linear spring linear spring magnetic-track relation, nonlinear stiffness magnetic-track relation and vehicle-electromagnetic force coupling magnetic-track relation research. The dynamics of the superconducting maglev vehicle are analyzed for three types of magnetic track relationships. In this way, the combination with a line-test comparison analysis provides an accurate approach to modeling the dynamics of superconducting maglev vehicle.

2 Superconducting Maglev System

The main components of the superconducting maglev system consists of three sets of coils, with the superconducting coil (hereinafter referred to as “SC coils”) mounted on both sides of the bogie and the traction coils and the levitation/guiding coils (hereinafter referred to as “LG coils”) installed on the U-track is shown in Figure 1.

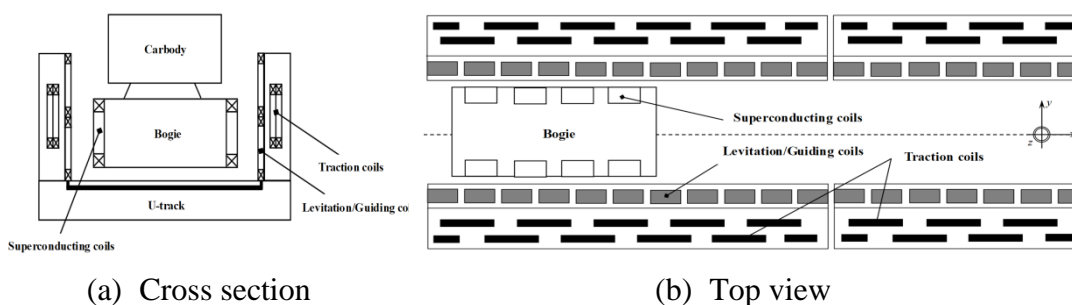


Figure 1: Superconducting maglev system.

The high magnetic field with alternating distribution of N- and S-pole generated by adjacent SC coils. And the traveling wave magnetic field generated by traction coil via ac control. The front traction coil is opposite to the magnetic pole of the superconducting coil, generating attraction, and the rear traction coil is the same as the magnetic pole of the superconducting coil, producing repulsion. The resulting

force from the front and rear actions drives the vehicle forward along the track direction.

The LG coils are composed of the "8" shaped coil connected by the upper and lower parts in series, which is not electrified. As the vehicle moves forward, the suspension coils cut the magnetic field of the SC coils, which in turn generates an induced current and induced magnetic field. The magnetic field generated by the lower half of LG coils repels the SC coils, while the magnetic field generated by the upper half of the LG coils attracts it. The upper and lower sections of the coils work together to form the electromagnetic force. The vehicle can be suspended when the vertical component of the electromagnetic force is equal to the gravity and the lateral component of the electromagnetic force on the two sides has a guiding effect on the vehicle operation and acts as a guiding force. The SC coils are installed on both sides of the track crossing line to form two sets of horizontal zero flux coils to further improve the guiding force of the system [9].

CRRC Changchun Railway Vehicles Co., Ltd has been focusing on superconducting electromagnetic technology research and built up the 200m straight test line with high temperature superconducting maglev vehicle of electric suspension system that includes acceleration, levitation and braking regions as shown in Figure 2. Acceleration area ground coils only install traction coils, provide longitudinal driving force for vehicles, into the levitation area, U-track add LG coils, provide vertical levitation force and lateral guiding force, into the brake area, vortex brake coils replacement for SC coils, superconducting maglev vehicles rely on electric brake and eddy current brake deceleration stop. The test system is modeled by a ratio size and equipped with high-temperature superconducting magnets. At the same time, the system integrates key subsystems such as safety control, diagnostic testing, speed measurement and localization, and wireless communication to ensure smooth and safe operation of the vehicle.

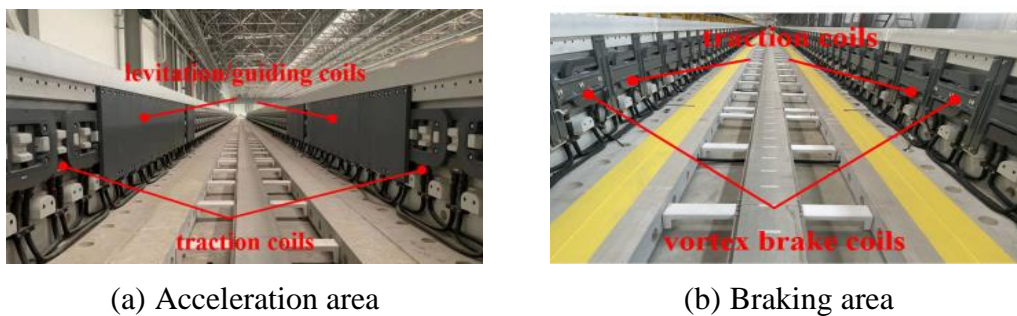


Figure 2: Superconducting maglev system.

3 Electromagnetic Force Characteristics and Magnetic Track Relations

Base on the KVL the equivalent circuit equation of the SC coils with crossing line is established [10].

$$\begin{bmatrix} R_{11} & R_{12} & 0 \\ R_{21} & R_{22} & R_{23} \\ 0 & R_{32} & R_{33} \end{bmatrix} \begin{bmatrix} I_1 \\ I_2 \\ I_3 \end{bmatrix} + \begin{bmatrix} M_{11} & M_{12} & 0 \\ M_{21} & M_{22} & M_{23} \\ 0 & M_{32} & M_{33} \end{bmatrix} \begin{bmatrix} \frac{dl_1}{dt} \\ \frac{dl_2}{dt} \\ \frac{dl_3}{dt} \end{bmatrix} = \begin{bmatrix} E_1 \\ E_2 \\ E_3 \end{bmatrix} \quad (1)$$

Column vector $[I_1, I_2, I_3]$ is loop current. Column vector $[E_1, E_2, E_3]$ is circuit electric potential. $[R_{11}, R_{12}, 0, R_{21}, R_{22}, R_{23}, 0, R_{32}, R_{33}]$ is resistor matrix. $[M_{11}, M_{12}, 0, M_{21}, M_{22}, M_{23}, 0, M_{32}, M_{33}]$ is inductive matrix.

Base on the neumann equation the equation of mutual sense coefficient solution is established.

$$dM_{dl_1, dl_2} = \frac{N_s N_g \mu_0}{4\pi} \oint_{l_2} \oint_{l_1} \frac{dl_1 \cdot dl_2}{R}, M_{1,2} = \sum_{i=1}^{j=1-p} dM_{dli, dlj} \quad (2)$$

dli, dlj is unit of segments divided by coil 1 and coil 2, respectively. n and p are the number of segments divided by coil 1 and coil 2, respectively. Define a matrix that describes all the building points of the coil. Base on the virtual work principle the equation of electromagnetic force is established [11].

$$F_i = \frac{\partial W}{\partial i} = I_s I_g \frac{\partial M}{\partial i}, i = x, x, y \quad (3)$$

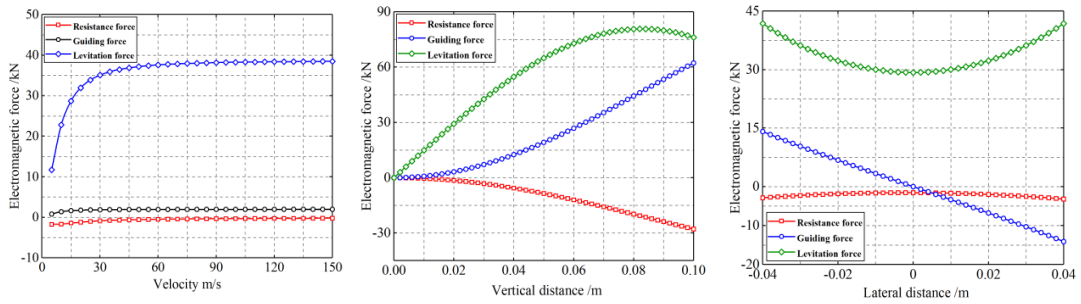
Combined with the above equations, the suspension force, guiding force and electromagnetic resistance of superconducting maglev are calculated as follows:

$$\begin{aligned} f_x &= \sum_{i=1}^m \sum_{j=1}^n I_s i_j \left(\frac{\partial M s_{i,j}}{\partial x} - \frac{\partial M s_{i,n+j}}{\partial x} \right) \\ &+ \sum_{i=1}^m \sum_{j=1}^n I_s i_{n+j} \left(\frac{\partial M s_{i,n+j}}{\partial x} - \frac{\partial M s_{m+i,2n+j}}{\partial x} \right) \\ &+ \sum_{i=1}^m \sum_{j=1}^n I_s i_{2n+j} \left(\frac{\partial M s_{m+i,2n+j}}{\partial x} - \frac{\partial M s_{m+i,3n+j}}{\partial x} \right) \end{aligned} \quad (4)$$

$$\begin{aligned} f_y &= \sum_{i=1}^m \sum_{j=1}^n I_s i_j \left(\frac{\partial M s_{i,j}}{\partial y_1} - \frac{\partial M s_{i,n+j}}{\partial y_1} \right) \\ &+ \sum_{i=1}^m \sum_{j=1}^n I_s i_{n+j} \left(\frac{\partial M s_{i,n+j}}{\partial y_1} - \frac{\partial M s_{m+i,2n+j}}{\partial y_2} \right) \\ &+ \sum_{i=1}^m \sum_{j=1}^n I_s i_{2n+j} \left(\frac{\partial M s_{m+i,2n+j}}{\partial y_2} - \frac{\partial M s_{m+i,3n+j}}{\partial y_2} \right) \end{aligned} \quad (5)$$

$$\begin{aligned}
f_z = & \sum_{i=1}^m \sum_{j=1}^n I_s i_j \left(\frac{\partial M s_{i,j}}{\partial z} - \frac{\partial M s_{i,n+j}}{\partial z} \right) \\
& + \sum_{i=1}^m \sum_{j=1}^n I_s i_{n+j} \left(\frac{\partial M s_{i,n+j}}{\partial z} - \frac{\partial M s_{m+i,2n+j}}{\partial z} \right) \\
& + \sum_{i=1}^m \sum_{j=1}^n I_s m+i i_{2n+j} \left(\frac{\partial M s_{m+i,2n+j}}{\partial z} - \frac{\partial M s_{m+i,3n+j}}{\partial z} \right)
\end{aligned} \tag{6}$$

Previous related studies have verified the correctness of the electromagnetic force model [12], which will not be demonstrated in detail in this paper. Figure 3 (a) shows the relation between velocity and electromagnetic force. As the superconducting maglev vehicle velocity is increased, the levitation and guiding force becomes larger. When the velocity reaches 50 m/s, the trend of the levitation and guiding force growth slows down and then reaches a saturation state. This is because by increasing the velocity, the speed of the magnetic field generated by the vehicle SC coils itself is cut by the track coil also increases, and the current generated by the induction gradually increases, making the levitation force continue to increase. When the velocity of the maglev vehicle increases again, the induced current rate generated inside the track coil also increases gradually, and the induced reactance generated inside the coil also increases rapidly, resulting in a smaller shift amplitude of the induced current, so that the electric suspension train can run stably in a stable state at a peak-speed stage. Figure 3 (b) shows the relation between vertical distance and electromagnetic force. As the superconducting maglev vehicle vertical distance is increased, the levitation and guiding force becomes larger first and then decreasing later. The levitation force reaches a maximum value at the vertical distance of 80 mm. There are similar rules for the guiding force. Figure 3 (c) shows the relation between lateral distance and electromagnetic force. Absolute value of the electromagnetic force with respect to the zero-point symmetry. As the superconducting maglev vehicle lateral distance is increased, the levitation force becomes larger. Also, there are similar rules for the guiding force.



(a) Velocity

(b) Vertical distance

(c) Lateral distance

Figure 3: The relationship between factors and electromagnetic force.

Calculate the system suspension force, guiding force, and magnetic resistance based on formula (4) ~ (6). We present three simplified models of the vertical

magnetic-track relationship to accommodate different simulation situations. Specifically, as shown in Figure 4 (a), when the system has minimal lateral amplitude and minor vertical fluctuations, the vertical magnetic-track relationship is reduced to a linear spring model (hereinafter referred to “model 1”). As shown in Figure 4 (b), when the system has minimal lateral amplitude and significant vertical fluctuations, the vertical magnetic-track relationship is reduced to a stiffness curve model (hereinafter referred to “model 2”). As shown in Figure 4 (c), when the system occurs significant lateral amplitude, the suspension force is related to the lateral and vertical distance that has obvious nonlinear characteristics. Simplifying the magnetic-track relations for dynamic simulation leads to larger errors. It is recommended to use the vehicle-electromagnetic force coupling model (hereinafter referred to “model 3”).

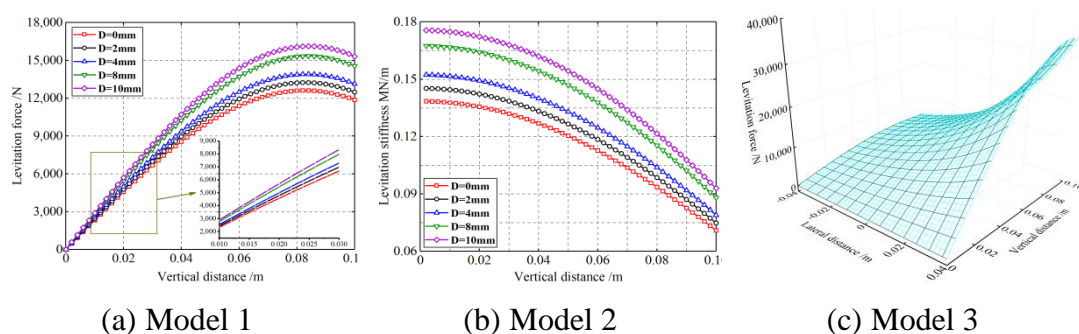


Figure 4: Vertical magnetic-track relations.

Meanwhile, we propose two simplified models of the lateral magnetic-track relations. As shown in Figure 5 (a), when the system has significant lateral amplitude and minimal vertical fluctuations, the lateral magnetic-track relationship is reduced to a stiffness curve model. As shown in Figure 5 (b), when the system has significant lateral amplitude and vertical fluctuation, the guiding force is related to the lateral and vertical fluctuation, which has obvious nonlinear characteristics. Simplifying the magnetic-track relationship for dynamic simulation leads to larger errors. It is recommended to use the vehicle-electromagnetic force coupling model.

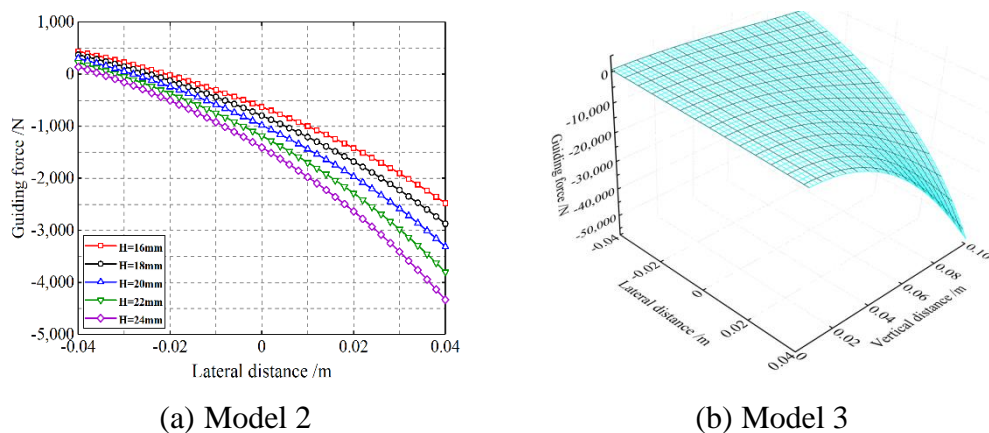


Figure 5: Lateral magnetic-track relations.

4 Maglev Vehicle Dynamic Simulations

As shown in Figure 6 (a) the new 200m straight test line with high temperature superconducting maglev vehicle built up in CRRC Changchun Railway Vehicles Co., Ltd which is mainly composed of bogie, carbody shell, support wheel, guide wheel, and four superconducting magnet mounted on both sides of the suspension frame, which provides the basis for the traction, levitation, guiding and braking of the vehicle. As shown in Figure 6 (b), according to the topology of the vehicle system, the simulation model of linear spring model, stiffness curve model and vehicle-electromagnetic force coupling dynamics model is established.

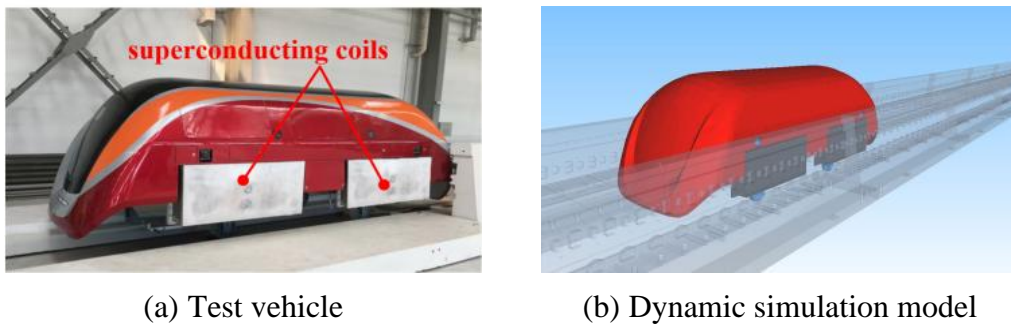
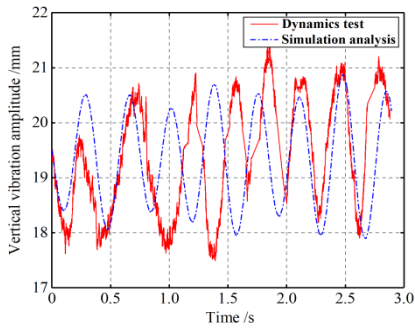


Figure 6: Simulation model of vehicle dynamics.

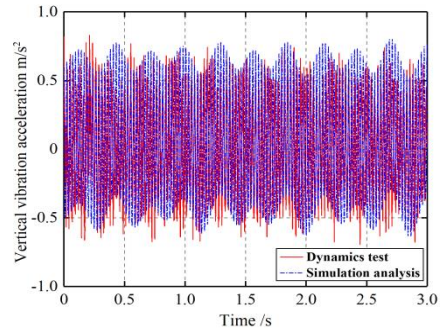
Figure 7 (a) indicates that when the electric suspension vehicle runs into the levitation areas, the vehicle starts levitating due to the electromagnetic force induced by the electromagnetic induction between the SC and LG coils. According to the data of the stable levitation stage, the displacement between the vertical center of the SC coils and that of the LG coils (hereinafter referred to as “balanced displacement”) is 19 mm, and the maximum vibration amplitude of the vehicle can reach 4 mm at this time. Dynamic simulations show that the stability balanced displacement is 19.5 mm, and entering the levitation areas, the vehicle vibration is minimal with an amplitude of 3 mm, which is consistent with the dynamic tests.

It should be especially emphasized that the fluctuation characteristics of vertical vibration amplitude of the dynamic simulated vehicle diverges slightly over time, which is consistent with the conclusion of the literature [13], which is caused by the small damping or negative damping characteristics of electric suspension. However, the fluctuating character of the vertical vibrational amplitude did not significantly diverge in the dynamical test, which could be caused by dissipative damping of the friction force between the guide wheel and the U-track during the levitation operation of superconducting maglev vehicle.

Figure 7 (b) indicates the comparison of vehicle vertical vibration acceleration under simulation analysis and dynamic test. The fluctuation characteristics of vertical vibration amplitude of the two modes agree with each other, which also confirms the correctness of the multi-DOF electromagnetic-vehicle coupled dynamics model.



(a) Vertical vibration amplitude

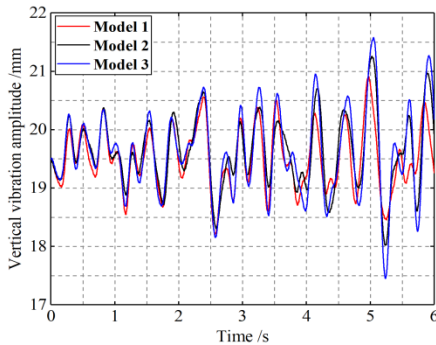


(b) Vertical vibration acceleration

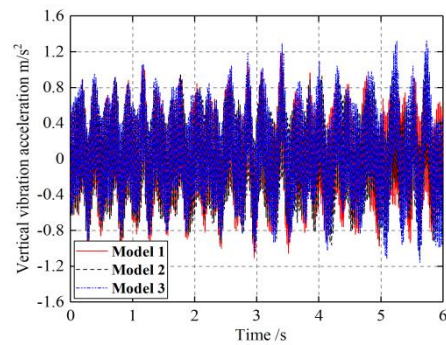
Figure 7: Comparison between line test and simulation analysis.

Based on the aforementioned lateral and vertical magnetic-track relationship, dynamic simulation models were developed and four simulation cases were constructed. Case 1 indicates minimal lateral amplitude and minor vertical fluctuations. Case 2 indicates minimal lateral amplitude and significant vertical fluctuations. Case 3 indicates significant lateral amplitude and minor vertical fluctuations. Case 4 indicates significant lateral amplitude and vertical fluctuations.

Figure 8 indicates the vertical dynamic response characteristics of the three kinds of magnetic-rail relationship models for working case 1. Model 3 has a slightly larger vertical vibration amplitude than Model 2 and a slightly larger amplitude than Model 1, with the relative difference being extremely minor. The vertical acceleration of the system at the same time has the same characteristic law.



(a) Vertical vibration amplitude



(b) Vertical vibration acceleration

Figure 8: Vertical dynamic response characteristics of the three kinds of models.

The vertical dynamic response characteristics of working case 1, case 2, case 3 and case 4 are listed in Table 1. When the vertical and lateral fluctuation amplitude of the system are minor, it is observed that the three magnetic-rail relationship models exhibit minimal errors and equivalent simulation accuracy. In cases where there is a certain degree of vertical fluctuation with minor lateral displacements, model 1 demonstrates significant error, while Model 2 and model 3 display equivalent simulation accuracy. Similarly, in scenarios involving a certain degree of lateral

amplitude but minimal vertical fluctuation, all three models for vertical characteristics exhibit negligible errors and equivalent simulation accuracy. But for lateral characteristics, model 2 has a large error. At this point, only model 3 can truly reflect the dynamical response of the system. However, when both lateral and vertical fluctuations are present simultaneously, it becomes evident that only model 3 can accurately capture the vertical and lateral dynamic response of the system as opposed to utilizing an equivalent magnetic-rail relations models.

Simulation condition	Magnetic-track relation model	Vertical amplitude (mm)	Vertical Acceleration (m/s^2)	Lateral amplitude (mm)	Lateral acceleration (m/s^2)
Case 1	Model 1	(18.20,20.90)	(-1.10,1.19)		
	Model 2	(18.00,21.30)	(-1.08,1.13)		
	Model 3	(17.70,21.60)	(-1.09,1.33)		
Case 2	Model 1	(19.70,22.41)	(-1.10,1.19)		
	Model 2	(16.82,21.85)	(-1.67,1.64)		
	Model 3	(16.87,22.65)	(-1.76,1.81)		
Case 3	Model 1	(18.20,20.90)	(-1.10,1.19)		
	Model 2	(18.00,21.30)	(-1.08,1.13)	(-7.90,8.30)	(-0.82,0.72)
	Model 3	(17.70,21.60)	(-1.19,1.33)	(-3.20,2.00)	(-0.73,0.75)
Case 4	Model 1	-	-	-	-
	Model 2	(16.80, 21.60)	(-1.68,1.64)	(-7.90,8.30)	(-0.82,0.77)
	Model 3	(16.20, 24.00)	(-2.00,2.04)	(-3.80,5.90)	(-0.76,0.75)

Table 1: Vertical dynamic response characteristics of four kinds of cases.

Figure 9 indicates the lateral dynamic response characteristics of the two kinds of magnetic-rail relationship models for working case 3. Model 2 has a slightly larger lateral vibration amplitude than Model 3. The lateral acceleration of the system at the same time has the same characteristic law.

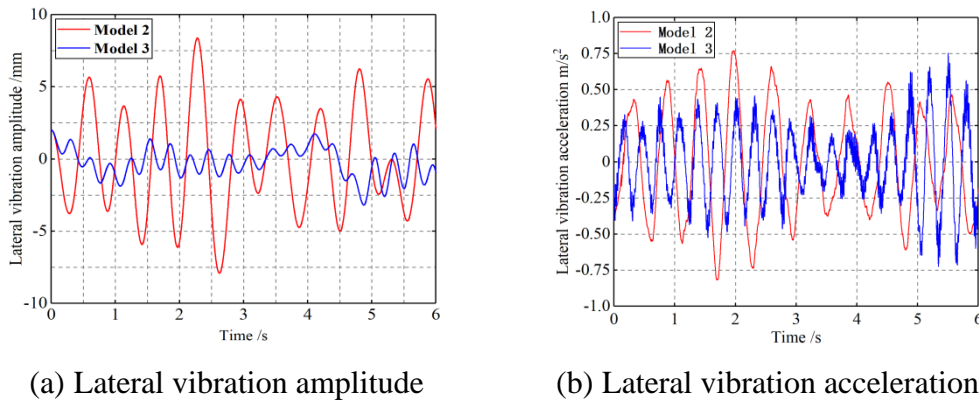


Figure 9: Lateral dynamic response characteristics of the two kinds of models.

The characteristics of the lateral dynamic response are listed in Table 2 for working cases 3 and 4. Once the system has a significant lateral amplitude, model 2 has a large error regardless of the presence of vertical fluctuations. At this point, only model 3 can truly reflect the dynamical response of the system.

Simulation condition	Magnetic-track relation model	Lateral amplitude (mm)	Lateral acceleration (m/s ²)
Case 1	Model 1	-	-
	Model 2	-	-
	Model 3	-	-
Case 2	Model 1	-	-
	Model 2	-	-
	Model 3	-	-
Case 3	Model 1	-	-
	Model 2	(-7.90,8.30)	(-0.82,0.72)
	Model 3	(-3.20,2.00)	(-0.73,0.75)
Case 4	Model 1	-	-
	Model 2	(-7.90,8.30)	(-0.82,0.77)
	Model 3	(-3.80,5.90)	(-0.76,0.75)

Table 2: Lateral dynamic response characteristics of two kinds of cases.

5 Conclusions

The magnetic-rail relation is an essential link between the maglev vehicle and the track and a crucial factor in ensuring the smooth and safe operation of the vehicle. In this paper, we have developed a circuit model based on superconducting maglev principle to solve electromagnetic force to carried out magnetic-rail relations for linear springs, nonlinear stiffness and coupling models. According to the new 200 m straight test line with high temperature superconducting maglev vehicle, the dynamic simulation models of three magnetic-rail relations are established. The magnetic-rail relation equivalent models are then chosen for different computational conditions.

The linear spring model can replace the nonlinear stiffness and coupling model as long as there is minimal lateral amplitude and minor vertical fluctuation. However, the linear spring model has significant errors when there is significant vertical fluctuation despite minor lateral amplitude. The stiffness curve model can only replace the coupling model for vertical characteristics when there is significant lateral amplitude and minor vertical fluctuation. Similarly, the equivalent magnetic-rail relations models have significant errors with larger lateral amplitude and vertical fluctuation.

References

- [1] JR. Powell, GT.Danby, "High speed transport by magnetically suspended trains", ASME Winter Annual Meeting, New York, 66-WA/RR-5. 1966.
- [2] M. Kim, JH. Jeong, J. Lim, et al. "Design and Control of Levitation and Guidance Systems for a Semi-High-Speed Maglev Train." *Journal of Electrical Engineering & Technology* 12.1(2017):117-125.
- [3] W. Bo, L. Shihu, W. Keren, et al. "Influence of different magnet-track relations on vertical dynamic performance of medium-low speed maglev vehicles." *Journal of Electric drive for locomotives* 5(2019):5 (in Chinese).
- [4] Hironori, et al. "Reduction of Vibrations in Maglev Vehicles Using Active Primary and Secondary Suspension Control." *Quarterly Report of Rtri* (2008).
- [5] K. Watanabe, et al. "A Study of Vibration Control Systems for Superconducting Maglev Vehicles." *Journal of System Design and Dynamics* 1.4(2007):703-713.
- [6] M. Nagai, A. Moran, S. Nakadai, "Study on Dynamic Stability of Repulsive Magnetic Levitation System (2nd Report, Vibration Control Effect of Active Secondary Suspension)." *Transactions of the Japan Society of Mechanical Engineers* 58.548(1992):1018-1023.
- [7] F. Piji, Z. Weihai, Z. Jingsong, et al. "Study on Fuzzy Improved Skyhook Control for Suspension Systems of Superconducting Electrodynamical Suspension Train." *Journal of the China Railway Society* 45.5(2023):47-56 (in Chinese).
- [8] Erimitsu, et al. "Comparison of Methods to Reduce Vibrations in Superconducting Maglev Vehicles by Primary Suspension Control." *Journal of Mechanical Systems for Transportation and Logistics* 1.1(2008):3-13.
- [9] H. JianLiang, D. M. Rote , H. T. Coffey, "Applications of the dynamic circuit theory to Maglev suspension systems." *IEEE Transactions on Magnetics* 29.6(1993):4153-4164.
- [10] L. Mili, V. Phaniraj, "Least median of squares estimation in power systems." *IEEE Transactions on Power Systems* 6.2(1991):511-523.
- [11] H. JianLiang, D. M. Rote, H. T. Coffey, "Applications of the dynamic circuit theory to Maglev suspension systems." *IEEE Transactions on Magnetics* 29.6(1993):4153-4164.
- [12] C. Dachuan, L. Xiaofen, et al. "An FEM Model for Evaluation of Force Performance of High-Temperature Superconducting Null-Flux Electrodynamical Maglev System." *IEEE Transactions on Applied Superconductivity*, 2021, 31(7): 1-6.
- [13] S. Ohashi, "Effect of the Active Damper Coils of the Superconducting Magnetically Levitated Bogie in Case of Acceleration." *IEEE Trans on Magnetics* 44.11(2008):4163-4166.